Histol Histopathol (2023) 38: 431-441

http://www.hh.um.es

Histology and Histopathology
From Cell Biology to Tissue Engineering

ORIGINAL ARTICLE **Open Access**

Circ_SATB2 knockdown inhibits the tumorigenesis of non-small cell lung cancer via miR-760/KIF2A axis

Pengchao Zheng*, Jianhua Jiang*, Lei Li, Liang Wei, Jie Li and Ling Jin

Cardio-Thoracic Surgery, Jing Men NO.2 People's Hospital, Jingchu University of Technology Affiliated Central Hospital, Jingmen, Hubei, China

*Pengchao Zheng and Jianhua Jiang contributed equally to this work

Summary. Purpose. This study was aimed at exploring the function and underlying mechanism of circ_SATB2 in non-small cell lung cancer (NSCLC).

Methods. The levels of circ_SATB2, microRNA-760 (miR-760) and Kinesin family member 2a (KIF2A) were determined using quantitative real-time polymerase chain reaction or western blot assay. The proliferation was detected using MTT and colony formation assays. Cell cycle and apoptosis were evaluated by flow cytometry. Transwell assay for migration and invasion and western blot for metastasis-associated proteins were conducted. Dual-luciferase reporter assay was used to analyze the interaction between miR-760 and circ_SATB2 or KIF2A. The effect of circ_SATB2 on NSCLC tumor growth *in vivo* was studied by xenograft mice model.

Results. Circ_SATB2 was upregulated in NSCLC tissues and cells. Circ_SATB2 knockdown caused inhibitory effects on NSCLC cell proliferation and metastasis but accelerated apoptosis. Circ_SATB2 served as a sponge of miR-760 to act in the development of NSCLC. Moreover, miR-760 could target KIF2A, and KIF2A expression was positively regulated by circ_SATB2. Furthermore, KIF2A overexpression neutralized miR-760-mediated inhibition effects on NSCLC cell progression. Besides, circ_SATB2 enhanced NSCLC tumorigenesis by targeting miR-760/KIF2A axis *in vivo*.

Conclusion. Circ_SATB2 was highly expressed and participated in the progression of NSCLC through the modulation of the miR-760/KIF2A axis, suggesting that circ_SATB2 might be a potential biomarker for the diagnosis of NSCLC.

Corresponding Author: Ling Jin, Cardio-Thoracic Surgery, Jing Men NO.2 People's Hospital, Jingchu University of Technology Affiliated Central Hospital, No.39 Xiangshan Avenue, Jingmen City, Hubei Province, 448000, PR China. e-mail: 13797959705@163.com

DOI: 10.14670/HH-18-530

Key words: Non-small cell lung cancer, circ_SATB2, miR-760, KIF2A

Introduction

Lung carcinoma (LC) is the most prevalent and deadliest malignancy that results in cancer-related death worldwide (Schwartz and Cote, 2016; Nasim et al., 2019). Although important advances in treatment and diagnosis of LC have been made in recent years (Jones and Baldwin, 2018), the reason for the high mortality rate of LC is still not fully explained. Therefore, exploring the potential mechanism and effective strategies for LC treatment is crucial.

Circular RNAs (circRNAs) possess covalent closed-loop structures and participate in gene regulation by serving as microRNA (miRNA) sponges (Panda, 2018). CircRNAs are involved in the biological and pathological processes of various diseases (Zhang et al., 2018), including LC (Huang et al., 2019). Circ_SATB2 (hsa_circ_0008928) had high expression in non-small cell lung carcinoma (NSCLC) tissues and cells, and participated in the progression of NSCLC cells via the miR-326/FSCN1 axis (Zhang et al., 2020). Nevertheless, the information about further functional mechanism of circ_SATB2 in NSCLC is lacking.

MiRNAs are endogenous, small non-coding RNAs that modulate posttranscriptional gene expression (Kabekkodu et al., 2018). The abnormal expression of miRNAs plays a pivotal part in LC etiology (Zarredar et al., 2018) and miRNAs are responsible for LC metastasis (Hashemi et al., 2017). A previous study has also confirmed that miR-760 was downregulated and might act as a tumor inhibitor in NSCLC (Wang and He, 2020). Meanwhile, Kinesin family member 2a (KIF2A) was upregulated and might serve as an oncogene in NSCLC tumorigenesis (Wang et al., 2020). However, the relation between miR-760 and KIF2A in NSCLC remains unexplored.

Here, this research investigated the abundance of

circ_SATB2 in NSCLC tissues and cells. Further, the function of circ_SATB2 in NSCLC and the interactions among circ_SATB2, miR-760 and KIF2A were investigated.

Materials and methods

Clinical samples

55 pairs of tumor tissues and adjacent healthy tissues from patients were procured from NSCLC patients enrolled at Jing Men NO.2 People's Hospital. All patients signed written informed consent and no patients accepted any therapy before surgery. This study protocol acquired the authorization of the Ethics Committee of Jing Men NO.2 People's Hospital.

Cell culture

Human NSCLC cell lines (H460 and H1299) and normal bronchial epithelial cell line (16HBE) were obtained from BeNa Culture Collection (Beijing, China). Cell culture was conducted in Dulbecco's modified Eagle's medium (DMEM; Gibco, Carlsbad, CA, USA) plus 10% fetal bovine serum (FBS; Gibco) and 1% antibiotics (Gibco) in a 5% CO_2 atmosphere at 37°C.

Quantitative real-time polymerase chain reaction (qRT-PCR)

The RNA was obtained via RNAiso Plus reagent (Takara, Dalian, China), and cDNA was synthesized by specific RT reagent kits (Takara). QRT-PCR reaction was conducted on a PCR system using SYBR Green (Invitrogen, Carlsbad, CA, USA). Relative expression was calculated exploiting the $2^{-\Delta\Delta Ct}$ method after normalization with reference glyceraldehyde-3-phosphate dehydrogenase (GAPDH) or U6. Special primer sequences were displayed as below: circ_SATB2, 5'-AGCCAACCAACTCTTCCGTG-3' (F) and 5'-AAAGCACATCTTTCCGCACC-3' (R); SATB2, 5'-CAAGAGTGGCATTCAACCGCAC-3' (F) and 5'-ATCTCGCTCCACTTCTGGCAGA-3' (R); miR-760, 5'-CGGCTCTGGGTCTGTG-3' (F) and 5'-GAACATGTCTGCGTATCTC-3' (R); KIF2A, 5'-GGCTGGAAATGAAAGAGGAG-3' (F) and 5'-CTTGCACGGAAAGGAGTATG-3' (R); GAPDH, 5'-TGACTTCAACAGCGACACCCA-3' (F) and 5'-CACCCTGTTGCTGTAGCCAAA-3' (R); U6, 5'-GCTTCGGCAGCACATATACTAAAAT-3' (F) and 5'-CGCTTCACGAATTTGCGTGTCAT-3' (R).

Ribonuclease R (RNase R) assay

Total RNA (5 μg) was exposed to 3 U/μg of RNase R (Lucigen, Middleton, WI, USA) or not (Mock) for 15 min at 37°C after RNA extraction from cells. The expression of circ_SATB2 and linear SATB2 was determined by qRT-PCR.

Subcellular fractionation location assay

The isolation of cytoplasmic and nuclear RNA from cells was conducted utilizing Nuclear or Cytoplasmic RNA Purification Kit (Fisher Scientific, Waltham, MA, USA). Then, the expression of circ_SATB2 in the nucleus and cytoplasm was examined by qRT-PCR with U6 or GAPDH serving as nuclear or cytoplasmic reference.

Cell transfection

Circ_SATB2 small interference RNA or lentiviral short hairpin RNA (si-circ_SATB2 or sh-circ_SATB2) and control si-NC or sh-NC, miR-760 mimic or inhibitor (miR-760 or anti-miR-760) and control miR-NC or anti-miR-NC, circ_SATB2 and KIF2A overexpression vectors (circ_SATB2 and KIF2A) and control pcDNA were all obtained from Ribobio (Guangzhou, China) and transfected into H460 and H1299 cells via Lipofectamine 3000 (Invitrogen).

Flow cytometry

For the determination of cell cycle distribution, transfected cells were collected and fixed with 70% ethanol at 4°C for 2h. The cell pellets were then incubated with propidine iodide (PI; BD Biosciences, San Diego, CA, USA) staining solution in the dark at 37°C for 10 min after being re-suspended in PBS (Gibco). Utilizing a flow cytometer, the distributed proportions of cells in different phases (G0/G1, S and G2/M) were obtained. For cell apoptosis detection, AnnexinV-FITC Apoptosis Detection Kit (BD Biosciences) was used following the manual. Subsequently, the apoptotic rate was identified by flow cytometer.

Colony formation assay

H460 and H1299 cells at 24h post-transfection were planted into 6-well plates and routinely maintained for 2 weeks. The colonies (>50 cells) were dyed with 1% crystal violet (Solarbio, Beijing, China) for 30 minutes after PBS washing and 4% paraformaldehyde (Solarbio) fixation. The colonies was counted with an inverted microscope.

MTT assay

H460 and H1299 cells were added into 96-well plates prior to transfection and incubated for different times. Then, each well was co-incubated with 10 μL MTT solution (Beyotime, Shanghai, China) for another 4 h, followed by DMSO (Solarbio) treatment to dissolve formazan. The optical density (OD) was determined at

570 nm by a microplate reader.

Transwell assays

Transwell chambers (Corning costar, Corning, NY, USA) were employed for the measurement of migratory and invasive cells, in which the chambers used for cell invasion were additionally pre-coated with Matrigel (Corning costar). H460 and H1299 cells in culture medium without FBS were plated into the upper chambers. Simultaneously, the lower chambers were added with complete medium plus 10% FBS. At 24h post-incubation at 37°C, the cells remaining on the surface of the upper chambers were discarded, and the transferred cells were immobilized with para-formaldehyde and dyed with crystal violet (all from Solarbio). The number of migratory and invasive cells in five randomly selected fields was counted under the microscope (amplification: 100 ×).

Western blot

Proteins were isolated utilizing RIPA lysis buffer (Beyotime). 30 μg protein was separated by 10% SDS-PAGE and then transferred onto PVDF membrane (Invitrogen). After blockage with 5% fat-free milk, the membranes were added with primary antibodies at 4°C overnight, followed by incubation with HRP-conjugated secondary antibody (ab205718; Abcam, Cambridge, MA, USA; 1: 3000) for 2h. The blots of protein bands were visualized by the enhanced chemiluminescence (ECL) detection kit (Millipore, Billarica, MA, USA). The antibodies were all acquired from Abcam and are listed as below: Snail (ab82846; 1: 500), E-cadherin (ab133597; 1: 2000), N-cadherin (ab207608; 1: 1000), vimentin (ab137321; 1: 2000), KIF2A (ab197988; 1: 1000) and control GAPDH (ab181602, 1:10000).

Dual-luciferase reporter assay

The wide type (WT) and mutated (MUT) sequences of circ_SATB2 or KIF2A 3'UTR containing the binding sites for miR-760 were cloned and inserted into pmirGLO reporter vector (Promega, Madison, WI, USA), termed as circ_SATB2-WT, KIF2A-WT, circ_SATB2-MUT or KIF2A-MUT. After transfecting these generated luciferase plasmids along with miR-760 or miR-NC into H460 and H1299 cells for 48h, the relative luciferase intensity was estimated via Dual-Luciferase Reporter Assay System (Promega).

Xenograft tumor model

5-week-old male BALB/c nude mice purchased from Beijing Vital River Laboratory Animal Technology Co., Ltd. (Beijing, China) were randomly divided into sh-NC group (n=6) and sh-circ_SATB2 group (n=6). H460 cells (2×10^6/200 μL PBS) stably expressing sh-circ_SATB2 or sh-NC were subcutaneously inoculated into the right flank of mice. The length and width of the tumors were measured every 5 days, and the volume of generated tumors was calculated by (length×width^2)/2. At 30 d post inoculation, all mice were euthanized and formed tumors were weighed. This study was authorized by the Animal Ethics Committee of Jing Men NO.2 People's Hospital.

Statistical analysis

Data from at least three duplicates were displayed as mean ± standard deviation and analyzed using SPSS 22.0 software. Difference comparison was conducted by Student's *t*-test or one-way analysis of variance. The correlation in tumor tissues among circ_SATB2, miR-760 and KIF2A levels was monitored by Spearman's correlation analysis. $P<0.05$ was identified as statistically significant.

Results

Circ_SATB2 was upregulated in NSCLC tissues and cells

Firstly, qRT-PCR result suggested that circ_SATB2 was significantly more overexpressed in NSCLC tumor tissues (n=55) than in adjacent normal tissues (n=55) (Fig. 1A). Also, circ_SATB2 was notably more highly expressed in NSCLC cells including H460 and H1299 cells than in normal 16HBE cells (Fig. 1B). Unlike the host gene SATB2 (linear mRNA), circ_SATB2 was resistant to RNase R digestion (Fig. 1C,D). Meanwhile, circ_SATB2 was mainly distributed in the cytoplasm of NSCLC cells (Fig. 1E,F).

Circ_SATB2 interference suppressed NSCLC cell proliferation, metastasis and induced cell apoptosis

As depicted in Fig. 2A,B, circ_SATB2 expression was visibly inhibited by si-circ_SATB2 transfection, while SATB2 expression was insusceptible in H460 and H1299 cells. Meanwhile, circ_SATB2 knockdown overtly facilitated cell cycle arrest at G0/G1 stage (Fig. 2C,D) and reduced the number of colonies (Fig. 2E) and cell proliferation (Fig. 2F,G) in H460 and H1299 cells. Further, cell apoptosis was distinctly enhanced (Fig. 2H) and cell migration and invasion were suppressed (Fig. 3A,B) in H460 and H1299 cells after si-circ_SATB2 transfection. Furthermore, the expression of metastasis-related proteins Snail, N-cadherin and vimentin was reduced while the expression of E-cadherin was elevated in H460 and H1299 cells after circ_SATB2 knockdown (Fig. 3C,D), which attested that circ_SATB2 silence impeded the metastasis process.

MiR-760 was a target of circ_SATB2 in NSCLC cells

Next, starbase database predicted that miR-760 had complementary sequence with circ_SATB2 (Fig. 4A).

The luciferase activity in H460 and H1299 cells co-transfected with circ_SATB2-WT and miR-760 was clearly decreased relative to miR-NC, but it remained unchanged in circ_SATB2-MUT group (Fig. 4B,C). Meanwhile, circ_SATB2 knockdown overtly enhanced miR-760 expression in H460 and H1299 cells (Fig. 4D). Besides, miR-760 was significantly lower expressed in NSCLC tissues and cells (Fig. 4E,F). Moreover, the expression of circ_SATB2 and miR-760 was negatively correlated in NSCLC tissues (Fig. 4G).

Silence of miR-760 partly reversed the effects of circ_SATB2 knockdown in NSCLC cell progression

Further, the cross-talk between circ_SATB2 and miR-760 was explored. Circ_SATB2 knockdown led to high expression of miR-760 in H460 and H1299 cells, while this upregulation was cancelled by anti-miR-760 addition (Fig. 5A). Functionally, the inhibitory effects of circ_SATB2 silence on the cell cycle progression (Fig. 5B,C), colony formation ability (Fig. 5D) and proliferation (Fig. 5E,F) were counteracted by the silence of miR-760. Furthermore, circ_SATB2 silence-triggered apoptosis in H460 and H1299 cells was also partly reversed by anti-miR-760 introduction (Fig. 5G). Besides, the suppressive effects of si-circ_SATB2 on migration and invasion were overturned by miR-760 silence (Fig. 5H,I). In addition, the reduced levels of Snail, N-cadherin and vimentin and the increased level of E-cadherin in H460 and H1299 cells transfected with si-circ_SATB2 were rescued with anti-miR-760 transfection (Fig. 5J,K).

MiR-760 directly interacted with KIF2A in NSCLC

Starbase database presented a potential binding sequence of miR-760 in KIF2A 3'UTR (Fig. 6A), and the reduced luciferase activity of KIF2A 3'UTR WT vector in H460 and H1299 cells transfected with miR-760 confirmed the direct interaction between them (Fig. 6B,C). Then, miR-760 was overexpressed or silenced with miR-760 mimic or anti-miR-760 (Fig. 6D). Expectedly, miR-760 overexpression dramatically reduced KIF2A expression, while miR-760 inhibition caused notable elevation in KIF2A level (Fig. 6E,F). Meanwhile, KIF2A was upregulated in NSCLC tissues (Fig. 6G,H) and cells (Fig. 6K,L), and its expression was negatively related to miR-760 expression, and positively associated with circ_SATB2 expression in NSCLC tissues (Fig. 6I,J). Moreover, KIF2A level was inhibited

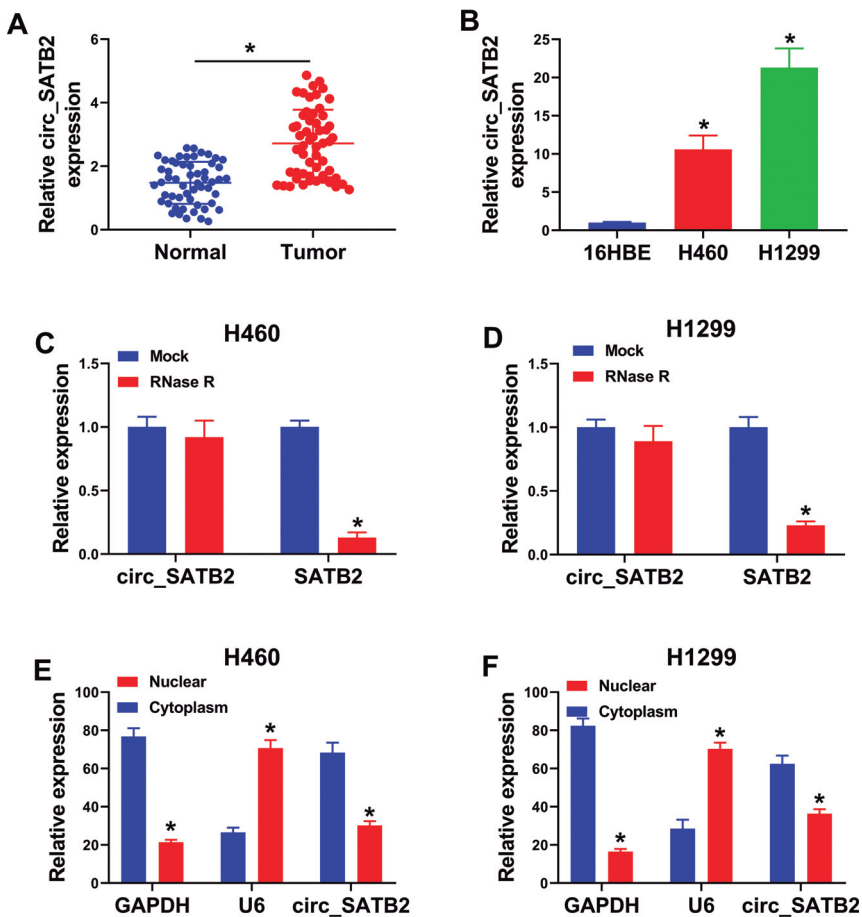

Fig. 1. Circ_SATB2 was highly expressed in NSCLC tissues and cells with a stable structure. **A, B.** The expression of circ_SATB2 in NSCLC tissues (n=55) and cells as well as normal tissues (n=55) and 16HBE cells was examined by qRT-PCR. **C, D.** The stability of circ_SATB2 and linear SATB2 was tested by RNase R assay. **E, F.** The distribution of circ_SATB2 in H460 and H1299 cells was attested by subcellular fractionation location assay. **P*<0.05.

by si-circ_SATB2 transfection, and increased again after anti-miR-760 addition (Fig. 6M,N).

MiR-760 suppressed the malignant behaviors of NSCLC cells through inhibiting KIF2A expression

To explore whether miR-760 targeted KIF2A to regulate NSCLC cell progression, miR-760 mimic and KIF2A overexpression vector were co-transfected into NSCLC cells. KIF2A overexpression significantly inverted the suppression effect of miR-760 on KIF2A mRNA and protein expression (Fig. 7A,B). Functional experiments revealed that miR-760 overexpression suppressed cell cycle progress, colony formation and viability in NSCLC cells, while these effects were overturned by KIF2A overexpression (Fig. 7C-G). MiR-760 mimic also promoted apoptotic rate, while it inhibited the number of migrated and invaded cells. However, these effects were reversed by KIF2A addition (Fig. 7H-J). Overexpressed miR-760 also increased E-cadherin protein expression and decreased the expression of Snail, N-cadherin and vimentin, while KIF2A overexpression revoked these effect (Fig. 7K,L). Above all, we confirmed that miR-760 inhibited NSCLC cell progression by targeting KIF2A.

Circ_SATB2 knockdown retarded NSCLC tumor growth in vivo

Lastly, H460 cell line stably transfected with sh-NC or sh-circ_SATB2 was used to establish the mice xenograft model. Our results showed that the tumor volume and weight were markedly reduced in the sh-circ_SATB2 group compared to the sh-NC group (Fig. 8A,B). Furthermore, we measured the expression of circ_SATB2 and miR-760 in the tumor tissues of each group, and found that circ_SATB2 abundance was reduced and miR-760 was upregulated in tumor tissues in sh-circ_SATB2 group (Fig. 8C,D). Besides, the mRNA and protein expression of KIF2A was also reduced in the tumor tissues of sh-circ_SATB2 group (Fig. 8E,F). Additionally, we discovered that E-cadherin protein expression was enhanced, while Snail, N-cadherin and vimentin protein expression levels were reduced in the tumor tissues of sh-circ_SATB2 group (Fig. 8G). Therefore, we confirmed that circ_SATB2 might promote NSCLC tumor growth through miR-760/KIF2A.

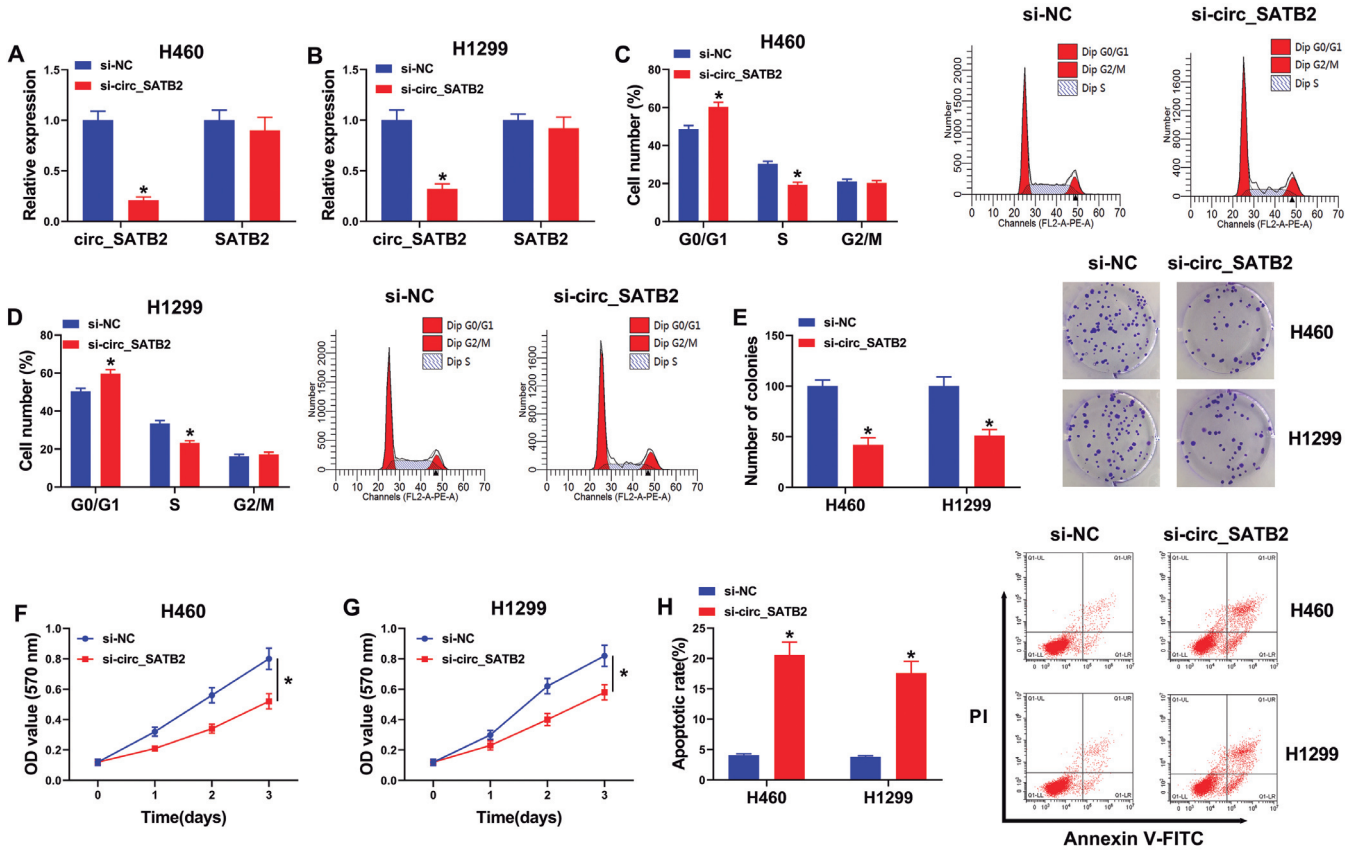

Fig. 2. Circ_SATB2 silence restrained the progression of NSCLC cells. H460 and H1299 cells were transfected with si-NC or si-circ_SATB2. **A, B.** QRT-PCR was utilized to test circ_SATB2 expression to confirm transfection efficiency. **C, D.** The percentage of H460 and H1299 cells in G0/G1, S or G2/M phase was analyzed by flow cytometry. **E.** The colony formation ability was evaluated by colony formation assay. **F, G.** The cell proliferation of transfected cells was assessed by MTT assay. **H.** Flow cytometry was used to assess the apoptosis rate in transfected group. **P*<0.05.

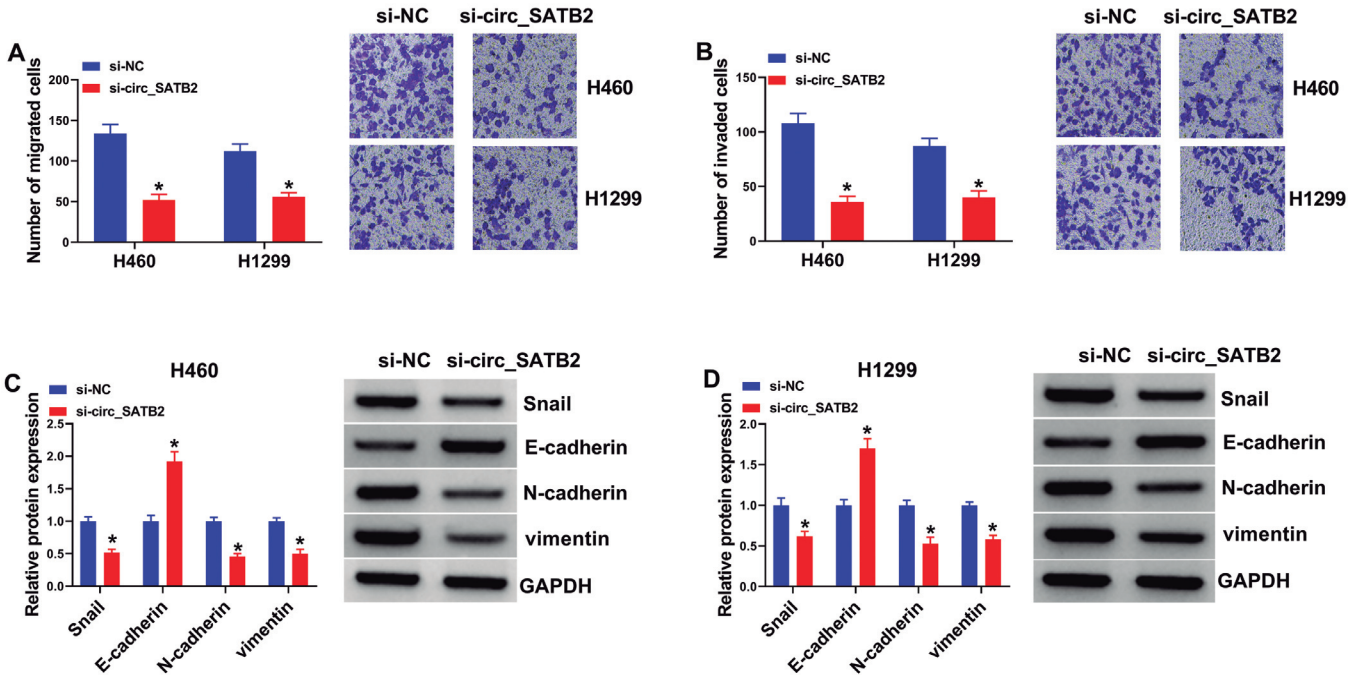

Fig. 3. Circ_SATB2 silence restrained NSCLC cell metastasis. **A, B.** The migration and invasion capacities were measured by transwell assays. **C, D.** The protein levels of metastasis-associated proteins (Snail, E-cadherin, N-cadherin and vimentin) were assessed by western blot. **P*<0.05.

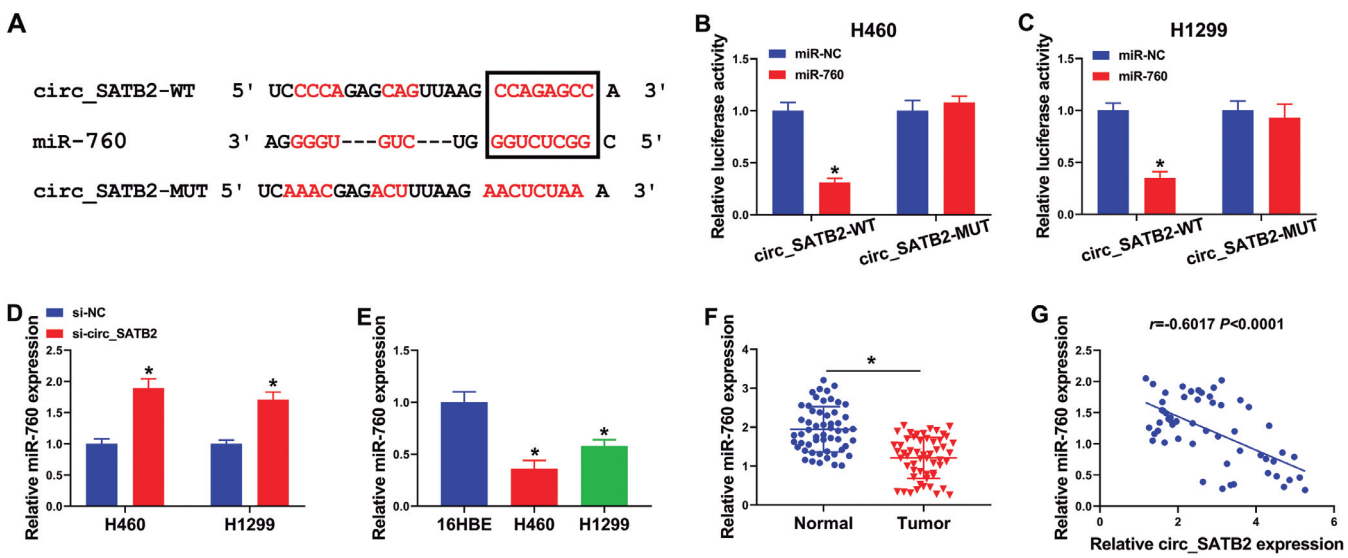

Fig. 4. Circ_SATB2 sponged miR-760. **A.** The putative binding sites between circ_SATB2 and miR-760 are shown. **B, C.** Dual-luciferase reporter assay was performed to verify the interaction between circ_SATB2 and miR-760. **D.** The expression of miR-760 in H460 and H1299 cells after circ_SATB2 knockdown was tested by qRT-PCR. **E.** miR-760 expression in H460 and H1299 cells and 16HBE cells was analyzed using qRT-PCR. **F.** miR-760 expression in NSCLC tissues and adjacent normal tissue was measured by qRT-PCR. **G.** The correlation between circ_SATB2 and miR-760 in NSCLC tissues was analyzed by Spearman's correlation analysis. **P*<0.05.

Discussion

Recently, many circRNAs have been reported to play pivotal role on monitoring tumor development in multifarious cancers (Zhang et al., 2018). Meanwhile, circRNAs can act as diagnostic biomarkers and new remedial targets for LC (Huang et al., 2019; Wang et al., 2019). In this study, the mechanism of the novel circRNA/miRNA/mRNA pathway based on circ_SATB2 was exposed in NSCLC etiology.

Mounting evidence has demonstrated that circRNAs are crucial regulatory molecules in the diverse biological processes of LC through the circRNA/miRNA regulatory network (Di et al., 2019; Liang et al., 2020). For example, circ_0007580 promotes NSCLC tumorigenesis by reducing miR-545-3p expression (Chen et al., 2020). Nevertheless, the studies about the role of circ_SATB2 in progression of cancers are few. Mao et al. demonstrated that circ_SATB2 was upregulated and modulated the proliferation and differentiation of vascular smooth muscle cells (VSMCs) through miR-939 (Mao et al.,

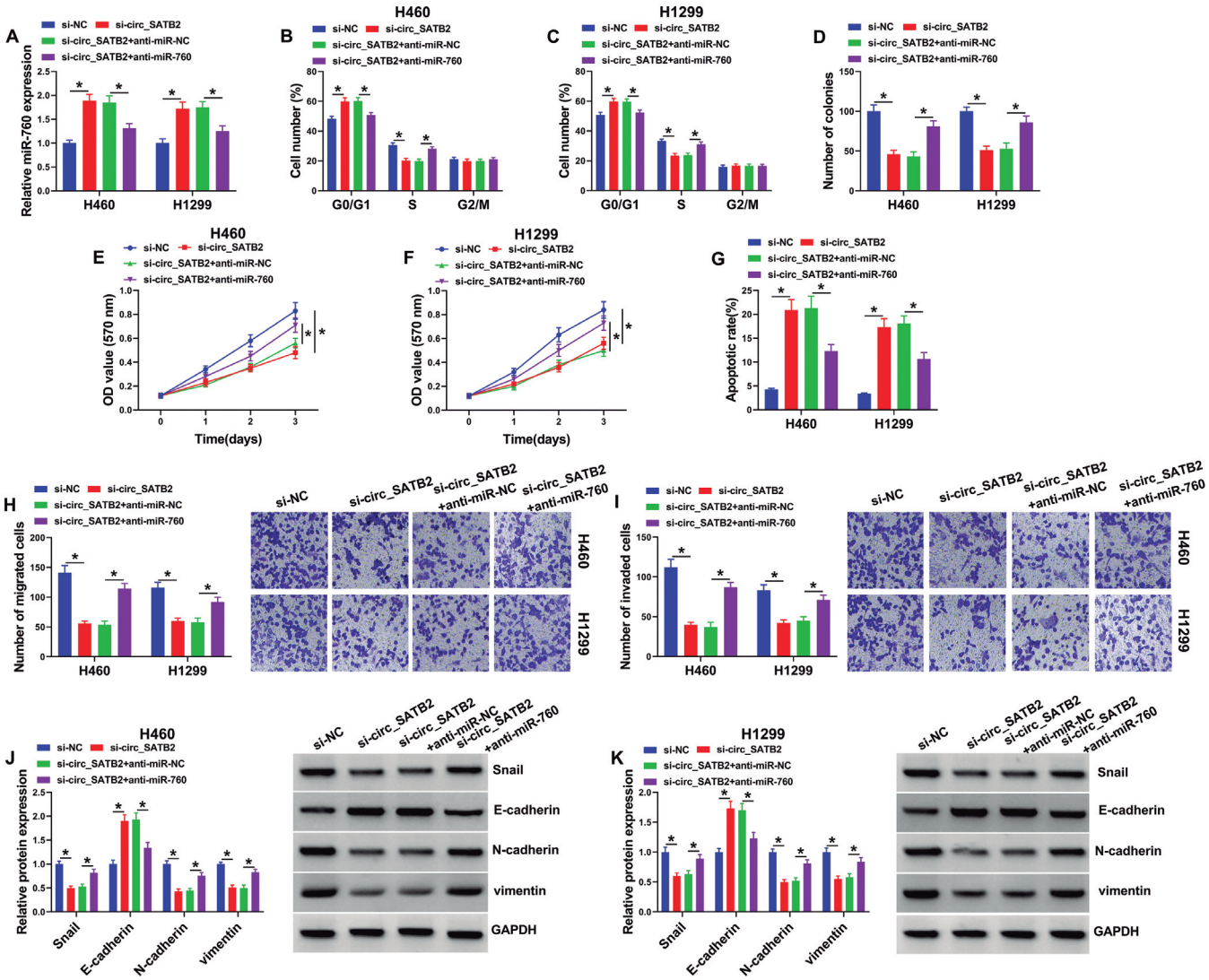

Fig. 5. The circ_SATB2/miR-760 axis regulated the progress of NSCLC cells. **A-K.** H460 and H1299 cells were transfected with si-NC, si-circ_SATB2, si-circ_SATB2+anti-miR-NC or si-circ_SATB2+anti-miR-760. **A.** The transfection efficiency of anti-miR-760 was confirmed by detecting miR-760 expression using qRT-PCR. **B, C.** The NSCLC cells in different phases of cell cycle (G0/G1, S and G2/M) were identified using flow cytometry. **D.** The number of visible colonies of H460 and H1299 cells was analyzed by colony formation assay. **E, F.** MTT assay was carried out to analyze the proliferation capacity of H460 and H1299 cells. **G.** The apoptotic rate of cells was determined by flow cytometry. **H, I.** Cell migration and invasion were tested by transwell assays. **J, K.** The metastatic abilities of H460 and H1299 cells were assessed through inspecting the levels of metastasis-associated proteins by western blot. *P<0.05.

2018). Meanwhile, circ_SATB2 was highly expressed and participated in NSCLC progression (Zhang et al., 2020). Similarly, this study validated that circ_SATB2 level was dramatically elevated in NSCLC tissues and cells. Functionally, circ_SATB2 knockdown might impede the proliferation and metastasis while accelerate

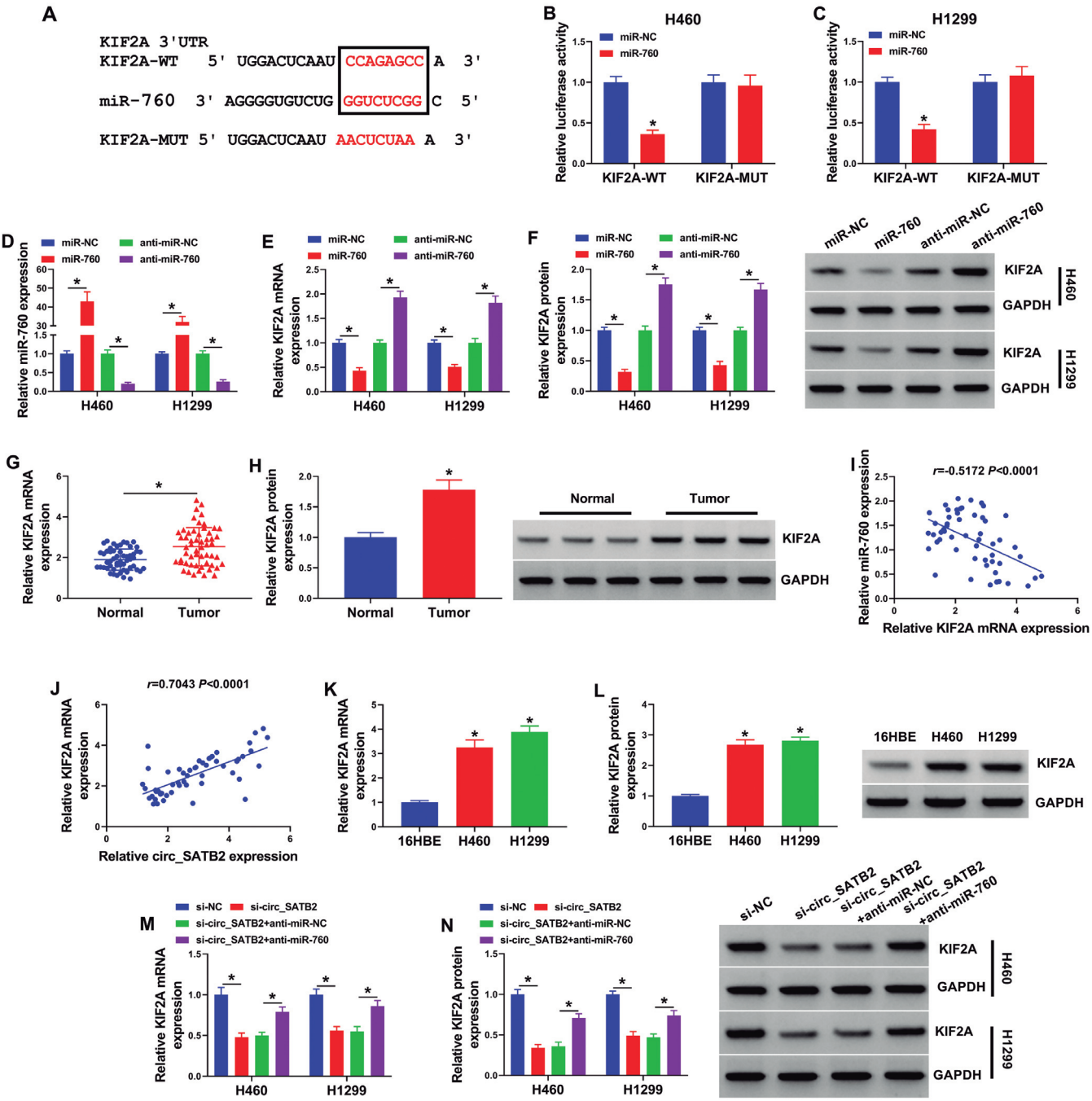

Fig. 6. MiR-760 interacted with the 3'UTR of KIF2A mRNA in NSCLC cells. **A.** The predicted KIF2A 3'UTR sequence with miR-760 and the corresponding mutant binding sites are presented. **B, C.** Dual-luciferase reporter assay was implemented to explore the interaction between KIF2A 3'UTR and miR-760. **D.** The overexpressed and silenced efficiencies of miR-760 in H460 and H1299 cells was examined by qRT-PCR. **E, F.** The mRNA and protein expression of KIF2A in H460 and H1299 cells transfected with miR-NC, miR-760, anti-miR-NC or anti-miR-760 was surveyed. **G, H.** The mRNA and protein abundances of KIF2A in NSCLC tissues and normal tissues were analyzed. **I, J.** Spearman's correlation analysis was used to analyze the correlation between KIF2A and miR-760 or circ_SATB2 in NSCLC tissues. **K, L.** The mRNA and protein levels of KIF2A in H460 and H1299 cells and normal 16HBE cells were determined. **M, N.** The mRNA and protein levels of KIF2A in H460 and H1299 cells transfected with si-NC, si-circ_SATB2, si-circ_SATB2+anti-miR-NC or si-circ_SATB2+anti-miR-760 were examined. **P*<0.05.

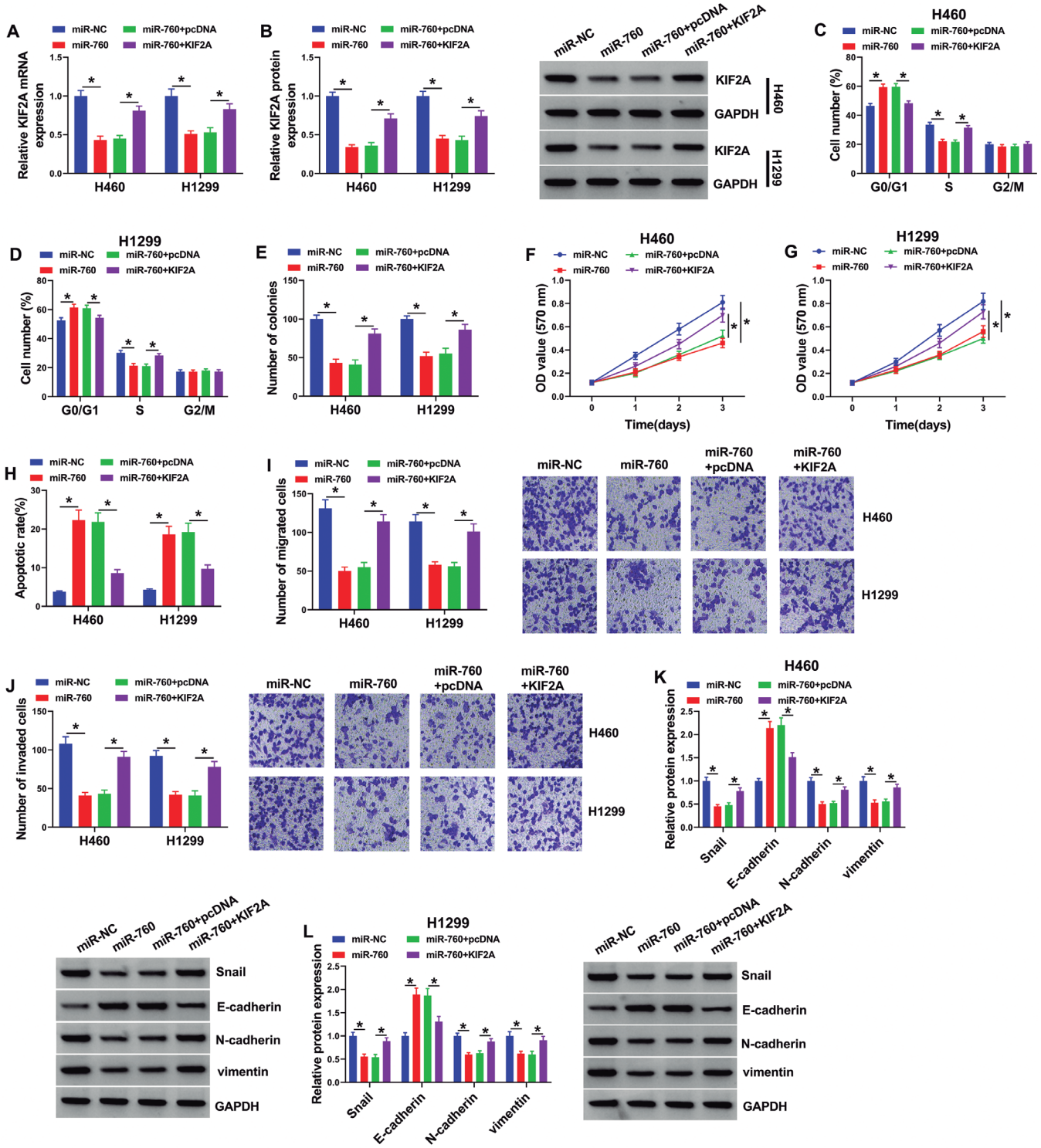

Fig. 7. The effects of miR-760 overexpression on the malignant potential of NSCLC was neutralized by KIF2A introduction. **A-L.** H460 and H1299 cells were transfected with miR-NC, miR-760, miR-760+pcDNA or miR-760+KIF2A. **A, B.** The mRNA and protein levels of KIF2A were tested by qRT-PCR and western blot. **C, D, H.** Flow cytometry analysis was implemented to detect cell cycle distribution and cell apoptosis. **E-G.** Colony formation assay and MTT assay were carried out to measure colony number and cell proliferative potential. **I, J.** The migration and invasion were determined by transwell assay. **K, L.** The protein levels of Snail, E-cadherin, N-cadherin and vimentin were analyzed by western blot. **P*<0.05.

apoptosis in NSCLC cells. Besides, circ_SATB2 silence was found to impede NSCLC tumor growth *in vivo* by regulating miR-760 and KIF2A. Therefore, we deduced that circ_SATB2 might accelerate the tumorigenesis and metastasis of NSCLC.

Compelling evidence has highlighted that miR-760 is downregulated and inhibits tumorigenesis in various cancers (Manvati et al., 2020), such as gastric cancer (Liu et al., 2020), hepatocellular carcinoma (Yin et al., 2020) and ovarian cancer (Li et al., 2020). Meanwhile, microRNAs have been corroborated to serve as pivotal tumor depressors in LC by base pairing with the 3'UTR of mRNA (Wu et al., 2019). For instance, miR-760 exhibited tumor-suppressive function in NSCLC progression through modulating SHCBP1 expression (Gao et al., 2020). In this study, miR-760 was lowly expressed in NSCLC tissues and cells, and it was forecasted to be targeted by circ_SATB2. Besides, there was a negative correlation between circ_SATB2 and miR-760 expression. Simultaneously, miR-760 depletion partly reversed the impacts of circ_SATB2 interference on the aggressive behaviors of NSCLC cells. Thus, circ_SATB2 might accelerate NSCLC progression through sponging miR-760.

Increasing evidence has announced that KIF2A was overexpressed and functioned as an oncogenic gene in lung-related cancer progression. For example, KIF2A silence blocked the propagation and facilitated apoptosis of lung adenocarcinoma cells (Xie et al., 2018). Furthermore, the aberrant expression of KIF2A promoted the cancer cell aggressiveness of lung squamous cell carcinoma (Uchida et al., 2019). In the present exploration, KIF2A level was verified to be raised in NSCLC tissues and cells, and it was targeted by miR-760. Meanwhile, miR-760 inhibited the malignant development of NSCLC cells, while the effects were neutralized by KIF2A overexpression. These data suggested that miR-760 might hinder NSCLC progression through sponging KIF2A. In addition, the decreased level of KIF2A induced by circ_SATB2 silence was reversed by miR-760 interference, hinting that circ_SATB2 might regulate KIF2A expression via absorbing miR-760. Together, all the data confirmed that circ_SATB2 participated in NSCLC tumorigenesis via the miR-760/KIF2A axis.

Conclusion

Circ_SATB2 contributed to the carcinogenesis of NSCLC by enhancing the miR-760-targeted KIF2A expression. This study proposed a circ_SATB2/miR-760/KIF2A regulatory axis in NSCLC etiology, and provided a potential therapeutic target for NSCLC remedy.

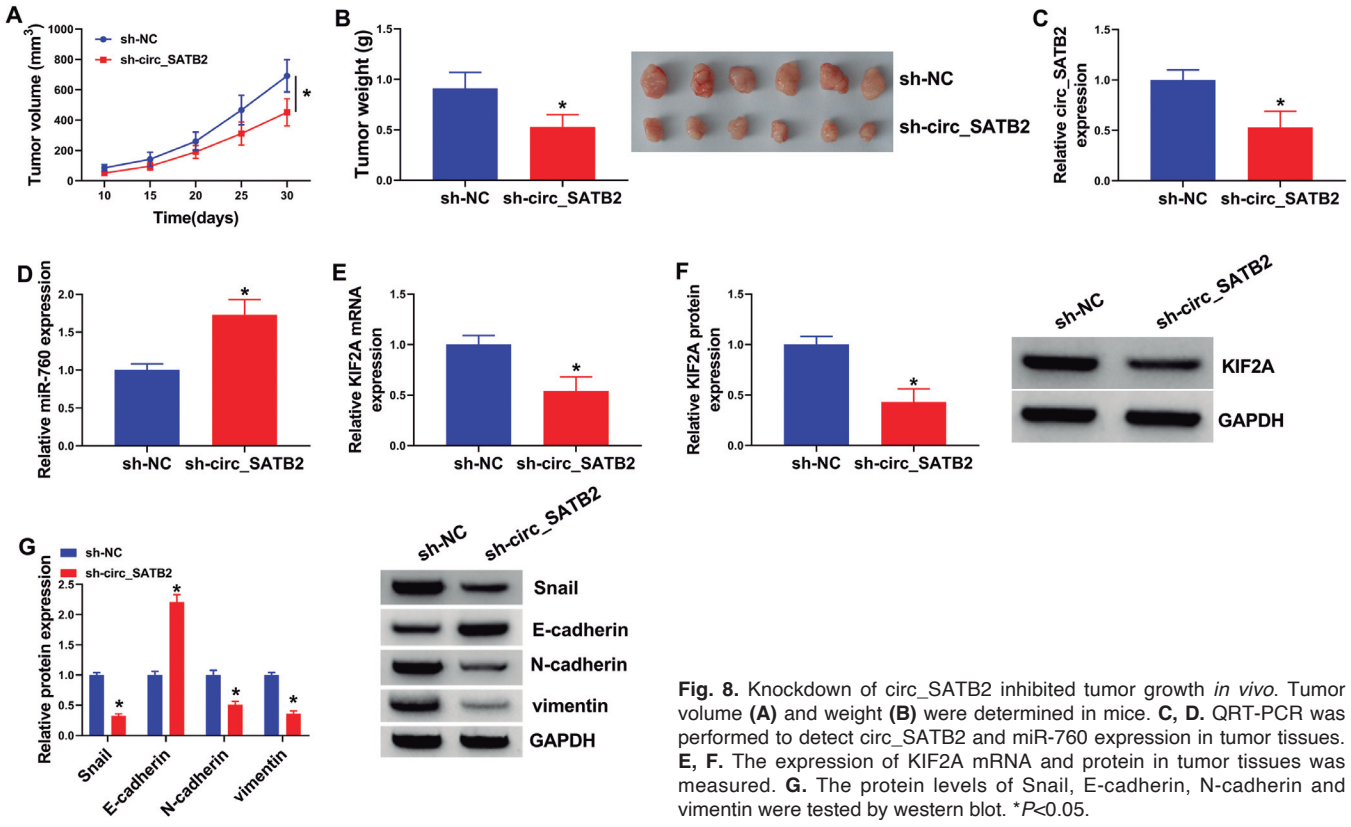

Fig. 8. Knockdown of circ_SATB2 inhibited tumor growth *in vivo*. Tumor volume **(A)** and weight **(B)** were determined in mice. **C, D.** QRT-PCR was performed to detect circ_SATB2 and miR-760 expression in tumor tissues. **E, F.** The expression of KIF2A mRNA and protein in tumor tissues was measured. **G.** The protein levels of Snail, E-cadherin, N-cadherin and vimentin were tested by western blot. **P*<0.05.

Acknowledgements. Not applicable.

Ethics approval and consent to participate. The present study was approved by the ethical review committee of Jing Men NO.2 People's Hospital. Written informed consent was obtained from all enrolled patients.

Consent for publication. Patients agreed to participate in this work.

Availability of data and materials. The analyzed data sets generated during the present study are available from the corresponding author on reasonable request.

Competing interests. The authors declare that they have no competing interests.

Funding. No funding was received.

References

Chen S., Lu S., Yao Y., Chen J., Yang G., Tu L., Zhang Z., Zhang J. and Chen L. (2020). Downregulation of hsa_circ_0007580 inhibits non-small cell lung cancer tumorigenesis by reducing miR-545-3p sponging. Aging (Albany NY) 12, 14329-14340.

Di X., Jin X., Li R., Zhao M. and Wang K. (2019). CircRNAs and lung cancer: Biomarkers and master regulators. Life Sci. 220, 177-185.

Gao W., Qi C.Q., Feng M.G., Yang P., Liu L. and Sun S.H. (2020). SOX2-induced upregulation of lncRNA LINC01561 promotes non-small-cell lung carcinoma progression by sponging miR-760 to modulate SHCBP1 expression. J. Cell Physiol. 235, 6684-6696.

Hashemi Z.S., Khalili S., Forouzandeh Moghadam M. and Sadroddiny E. (2017). Lung cancer and miRNAs: a possible remedy for anti-metastatic, therapeutic and diagnostic applications. Expert Rev. Respir. Med. 11, 147-157.

Huang X., Zhang W. and Shao Z. (2019). Prognostic and diagnostic significance of circRNAs expression in lung cancer. J. Cell Physiol. 234, 18459-18465.

Jones G.S. and Baldwin D.R. (2018). Recent advances in the management of lung cancer. Clin. Med. (Lond) 18, s41-s46.

Kabekkodu, S.P., Shukla, V., Varghese, V.K., J, D.S., Chakrabarty, S. and Satyamoorthy, K. (2018). Clustered miRNAs and their role in biological functions and diseases. Biol. Rev. Camb Philos. Soc. 93, 1955-1986.

Li L., Yu P., Zhang P., Wu H., Chen Q., Li S. and Wang Y. (2020). Upregulation of hsa_circ_0007874 suppresses the progression of ovarian cancer by regulating the miR-760/SOCS3 pathway. Cancer Med. 9, 2491-2499.

Liang Z.Z., Guo C., Zou M.M., Meng P. and Zhang T.T. (2020). circRNA-miRNA-mRNA regulatory network in human lung cancer: an update. Cancer Cell Int. 20, 173.

Liu W., Li Y., Feng S., Guan Y. and Cao Y. (2020). MicroRNA-760 inhibits cell viability and migration through down-regulating BST2 in gastric cancer. J. Biochem. 168, 159-170.

Manvati M.K.S., Khan J., Verma N. and Dhar P.K. (2020). Association of miR-760 with cancer: An overview. Gene 747, 144648.

Mao Y.Y., Wang J.Q., Guo X.X., Bi Y. and Wang C.X. (2018). Circ-SATB2 upregulates STIM1 expression and regulates vascular smooth muscle cell proliferation and differentiation through miR-939. Biochem. Biophys. Res. Commun. 505, 119-125.

Nasim F., Sabath B.F. and Eapen G.A. (2019). Lung cancer. Med. Clin. North. Am. 103, 463-473.

Panda A.C. (2018). Circular RNAs Act as miRNA sponges. Adv. Exp. Med. Biol. 1087, 67-79.

Schwartz A.G. and Cote M.L. (2016). Epidemiology of lung cancer. Adv. Exp. Med. Biol. 893, 21-41.

Uchida A., Seki N., Mizuno K., Yamada Y., Misono S., Sanada H., Kikkawa N., Kumamoto T., Suetsugu T. and Inoue H. (2019). Regulation of KIF2A by antitumor miR-451a inhibits cancer cell aggressiveness features in lung squamous cell carcinoma. Cancers (Basel) 11, 258.

Wang W. and He B. (2020). MiR-760 inhibits the progression of non-small cell lung cancer through blocking ROS1/Ras/Raf/MEK/ERK pathway. Biosci. Rep. 29, BSR20182483.

Wang C., Jiang Y., Lei Q., Wu Y., Shao J., Pu D. and Li W. (2019). Potential diagnostic and prognostic biomarkers of circular RNAs for lung cancer in China. Biomed. Res. Int. 2019, 8023541.

Wang G., Wang Z. and Yu H. (2020). Kinesin family member 2A high expression correlates with advanced tumor stages and worse prognosis in non-small cell lung cancer patients. J. Clin. Lab. Anal. 34, e23135.

Wu K.L., Tsai Y.M., Lien C.T., Kuo P.L. and Hung A.J. (2019). The roles of microRNA in lung cancer. Int. J. Mol. Sci. 20, 1611.

Xie T., Li X., Ye F., Lu C., Huang H., Wang F., Cao X. and Zhong C. (2018). High KIF2A expression promotes proliferation, migration and predicts poor prognosis in lung adenocarcinoma. Biochem. Biophys. Res. Commun. 497, 65-72.

Yin L., Sun T. and Liu R. (2020). NACC-1 regulates hepatocellular carcinoma cell malignancy and is targeted by miR-760. Acta Biochim. Biophys. Sin. (Shanghai) 52, 302-309.

Zarredar H., Ansarin K., Baradaran B., Shekari N., Eyvazi S., Safari F. and Farajnia S. (2018). Critical microRNAs in lung cancer: Recent advances and potential applications. Anticancer Agents Med. Chem. 18, 1991-2005.

Zhang H.D., Jiang L.H., Sun D.W., Hou J.C. and Ji Z.L. (2018). CircRNA: a novel type of biomarker for cancer. Breast Cancer 25, 1-7.

Zhang N., Nan A., Chen L., Li X., Jia Y., Qiu M., Dai X., Zhou H., Zhu J., Zhang H., et al. (2020). Circular RNA circSATB2 promotes progression of non-small cell lung cancer cells. Mol. Cancer 19, 101.

Accepted October 5, 2022